BMC Genomics

RESEARCH

Open Access

Short-term heat exposure affects thermogenesis and mitophagy in goat brown adipocytes

Yulong Song[1,2,3], Die Li[1,2,3], Duo Su[1,2,3], Tingting Jiang[1,2,3], Longrui Li[1,2,3], Siyuan Zhan[1,2,3], Tao Zhong[1,2,3], Jiazhong Guo[1,2,3], Jiaxue Cao[1,2,3], Li Li[1,2,3], Hongping Zhang[1,2,3] and Linjie Wang[1,2,3*]

Abstract

Background Brown adipose tissue (BAT) has a significant impact in newborn goats on maintaining body temperature through non-shivering thermogenesis in response to cold exposure. However, the roles of heat treatment on BAT thermogenesis are still limited.

Results This study focused on the effects of short-term heat exposure on goat brown adipocytes. We found that the content of mitochondria and the proteins of UCP1 and PGC1α were increased after 12 h of heat exposure. Additionally, the triglyceride (TG) content was significantly decreased after 1, 2, 6 h of heat exposure. Furthermore, RNA-seq analysis of brown adipocytes after 12 h of heat exposure identified 1091 differentially expressed genes (DEGs). The KEGG enrichment analysis were mainly enriched in thermogenesis, fatty acid metabolism and mitophagy. In addition, we found that the amount of mitophagosomes and expression levels of mitophagy-related protein (LC3BII/LC3BI, BNIP3, and BECN) were elevated after 12 h of heat treatment.

Conclusion These findings collectively indicate that heat exposure enhances the thermogenic capacity and mitophagy level of goat brown adipocytes. Our study provides evidence that heat exposure facilitates adaptive thermogenesis in goat brown adipocytes.

Keywords Goat, Brown adipocytes, Thermogenesis, Lipogenesis, Heat exposure, Mitophagy

Introduction

Adipose tissues can be divided into three categories: white, brown, and beige. Brown adipose tissue (BAT) has a typical multi-chamber structure and a higher number of mitochondria, which can be used to produce heat by uncoupling the oxidative phosphorylation from ATP generation through uncoupling protein 1 (UCP1) [1, 2]. Brown adipose tissues are mainly distributed in the interscapular, pericardiac, and perirenal regions of newborn lambs and goats to maintain core body temperature. The amount of BAT is highest at birth and converts into white adipose tissue (WAT) over the course of 30 d post birth [3–5].

*Correspondence:
Linjie Wang
wanglinjie@sicau.edu.cn
[1]Key Laboratory of Livestock and Poultry Multi-omics, Ministry of Agriculture and Rural Affairs, College of Animal Science and Technology, Sichuan Agricultural University, Chengdu, Sichuan 611130, P. R. China
[2]Farm Animal Genetic Resources Exploration and Innovation Key Laboratory of Sichuan Province, College of Animal Science and Technology, Sichuan Agricultural University, Chengdu, Sichuan 611130, P. R. China
[3]Key Laboratory of Agricultural Bioinformatics, Ministry of Education, Sichuan Agricultural University, Chengdu, Sichuan 611130, P. R. China

Cold stimulation activates the non-shivering thermogenesis of BAT via the hypothalamic-pituitary-adrenal axis (HPA) [6]. Norepinephrine (NE) stimulates β3-adrenergic receptors on the surface of brown adipocytes and then activates the thermogenesis process [2]. It has been reported that the body temperature decreases rapidly in lambs after birth [7], and the survival rate of lambs decreases with the loss of heat [8, 9]. In addition, the non-shivering thermogenesis of BAT could generate ~ 50% of the total thermogenesis and protect lambs from cold [10, 11]. Therefore, improving the thermogenesis ability of BAT is beneficial for lambs and goat kids to respond to cold conditions. In our prior studies, we have discovered that cold stimulation induces BAT thermogenesis in goat kids and increases the expression of thermogenic genes [12]. Moreover, the maternal supplementation of L-carnitine enhances the BAT thermogenesis of goat kids after cold exposure [13]. Supplementation of copper also increases the expression of *UCP1* and leads to higher amounts of mitochondria with fewer lipid droplets in BAT [14] and maternal injection of L-arginine can elevate thermogenesis capacity of BAT in lambs [15]. Interestingly, recent evidence suggests that external heat exposure could also activate brown and beige adipose tissues. It has been shown that local hyperthermia therapy induces the thermogenesis of beige adipose and enhances the expression of thermogenic genes in brown adipose tissues in both mice and humans [16]. However, studies on heat exposure on goat BAT thermogenesis are still limited.

When the ambient temperature exceeds the optimal temperature for livestock, the heat exposure occurs, leading to potential physiological stress and changes in metabolic processes [17, 18]. For in vitro brown adipocytes, it has been reported that heat shock proteins and thermosensitive transient receptor potential (TRP) channels form a temperature-sensing system [19]. For our study, we used BAT-derived stromal vascular fraction (SVF), which can be differentiated into functional brown adipocytes [20], providing a reliable model for studying their responses to external thermal exposure. Based on previous research about heat exposure on adipocytes [16, 21–24], we constructed a heat exposure model for goat brown adipocytes and selected different durations of heat exposure to investigate the effects of heat exposure, particularly short-term heat exposure, on thermogenesis, adipogenesis, and mitophagy in goat brown adipocytes.

In this study, we performed heat exposure on goat brown adipocytes and found that the content of mitochondria was raised and the expression of thermogenesis genes was also up-regulated. The adipocytes lipogenesis and lipolysis were also activated. In addition, we demonstrated that heat exposure induced thermogenesis and activated mitophagy pathways by RNA-seq analysis in goat brown adipocytes. Our study provides evidence supporting the role of heat exposure in promoting adaptive thermogenesis in goat brown adipocytes.

Results

Identification of goat brown adipocytes

To evaluate whether the SVFs separated from brown adipose tissues of newborn goat kids can differentiate into mature brown adipocytes, we determined the brown adipocytes marker genes, including *UCP1*, *PGC1α*, *CPT1A*, *ELOVL3*, and *ELOVL6* (Fig. 1A). After 8 d of browning differentiation, the mRNA levels of marker genes were significantly increased ($p < 0.05$) compared with undifferentiated cells. Except qPCR, we also performed UCP1 immunocytochemistry and lipid stain on goat brown adipocytes (Fig. 1B). We found that abundant lipid droplets and UCP1 expression in goat mature brown adipocytes. These results indicate that the SVFs separated from goat brown adipose tissues are capable of being induced into brown adipocytes.

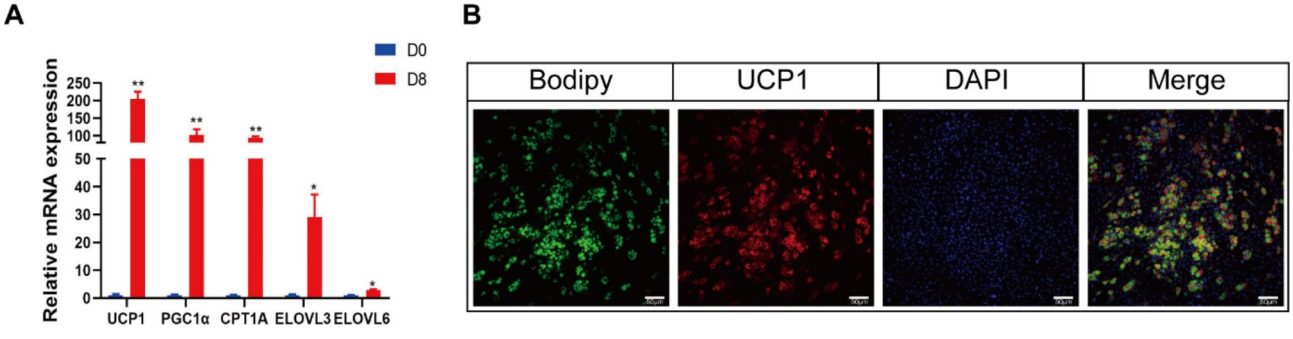

Fig. 1 Identification of goat brown adipocytes. (**A**) The mRNA expression level of brown adipocytes marker genes in undifferentiated cells (D0) and after 8 d of differentiation (D8) ($n = 6$). (**B**) BODIPY staining of lipid droplets and immunocytochemistry staining of UCP1 in brown adipocytes at D8 (scale bar = 50 μm). Data are presented as mean ± SEM. *$p < 0.05$ and **$p < 0.01$ versus the corresponding controls are indicated

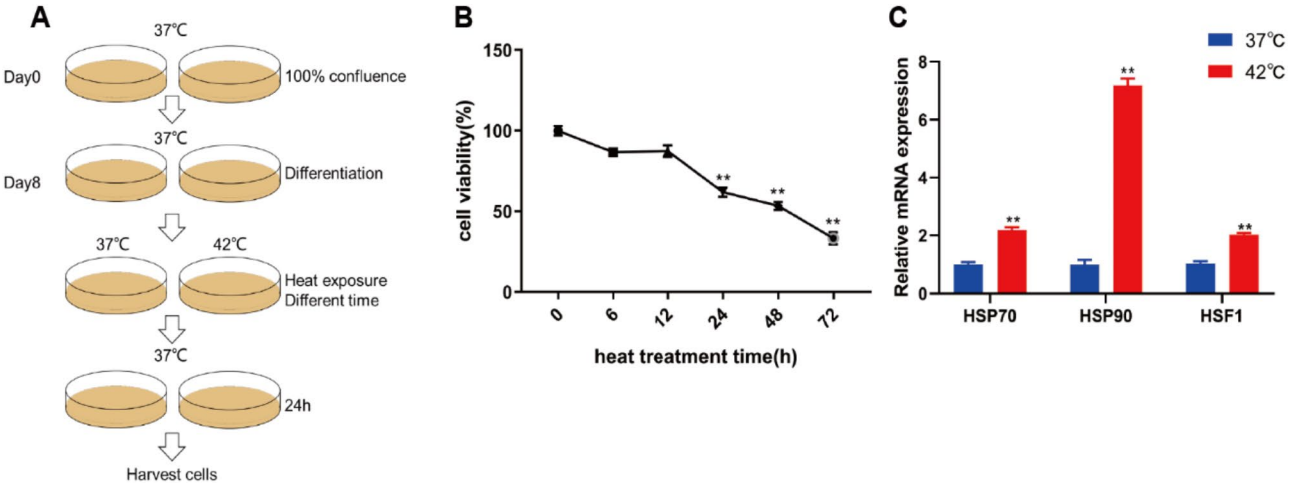

Fig. 2 Heat exposure affects cell viability and elevates the expression of heat shock genes. (**A**) Schematic figure of cell culture and different heat treatment time; (**B**) Cellular viability of goat brown adipocytes after different heat treatment time (42℃, $n=6$). (**C**) The mRNA expression levels of heat shock genes of brown adipocytes in 37℃ and exposed to 42℃ for 12 h ($n=6$). Data are presented as mean ± SEM. *$p<0.05$ and **$p<0.01$ versus the corresponding controls are indicated

Heat exposure affects cellular viability and elevates the expression of heat shock protein genes

Brown adipocytes were treated at 42℃ for different times and put back to 37℃ for 24 h (Fig. 2A). Then, we used the CCK-8 kit to determine whether cellular viability was affected by heat exposure. We found that cellular viability did not change after 6 and 12 h treatment. In addition, cellular viability was significantly lower compared with control after 24, 48, and 72 h of heat exposure ($p<0.05$) (Fig. 2B). The results indicated that the 12 h of heat exposure was the longest treatment time without affecting cellular viability. Therefore, we selected 42℃ for 12 h as the heat treatment condition for subsequent experiments.

To determine whether the heat exposure model of goat brown adipocytes was built, we examined the gene expression levels of heat shock proteins (*HSP70* and *HSP90*) and heat shock factor 1 (*HSF1*). These genes were significantly up-regulated after 12 h of heat exposure ($p<0.05$) (Fig. 2C), which represented that the heat exposure model was established in goat brown adipocytes.

Heat exposure induces thermogenesis of goat brown adipocytes

To investigate whether heat exposure regulates the thermogenesis of brown adipocytes, we used the mitotracker to stain the mitochondria and the copy number of mitochondria was determined by qPCR. The results show that the content of mitochondria was increased after 12 h heat exposure ($p<0.05$) (Fig. 3A-C). Then, heat exposure significantly induced the expression levels of thermogenesis related genes including *UCP1*, *PGC1α*, and *CPT1A* ($p<0.05$) (Fig. 3D), as well as the level of UCP1 and PGC1α proteins compared with the control group ($p<0.05$) (Fig. 3E and F).

Heat exposure affects lipogenesis and lipolysis of brown adipocytes

To further verify whether heat exposure regulates the lipid accumulation of brown adipocytes, oil-red O was used for dyeing lipid droplets. We found that the concentration of TG was significantly decreased ($p<0.05$) after 1, 2, and 6 h of heat exposure (Fig. 4A and B). Interestingly, there was no apparent change between 0 h and 12 h heat exposure. Therefore, we detected the expression of lipogenesis genes including *PPARγ*, *FABP4*, and *FASN* (Fig. 4C). *PPARγ* was significantly reduced after 1 h of heat exposure ($p<0.05$), while FABP4 and FASN were significantly down-regulated at 1 h and at 1, 2 h, respectively ($p<0.05$). Furthermore, *FABP4* and *FASN* were significantly up-regulated after 12 h of heat exposure ($p<0.05$). We also determined *ATGL*, the key gene of lipolysis. It was also significantly increased after heat exposure for 1, 2, 6, and 12 h ($p<0.05$) (Fig. 4C). These results demonstrate that the lipogenesis and lipolysis of brown adipocytes are promoted after 12 h heat exposure.

RNA-seq reveals the regulatory roles of heat exposure on goat brown adipocytes

To determine the alteration of gene expression patterns after heat exposure, we performed RNA-seq on the goat brown adipocytes that incubated at 37℃ and 42℃ after 12 h heat exposure (Fig. 5A). We examined gene expression patterns with PCA, which showed that the HE and NC samples clustered into distinct group (Fig. 5B). In further RNA-seq analysis, we found a total of 1091 differential expression genes (DEGs), of which 582 were up-regulated and 509 were down-regulated (Fig. 4C). The KEGG enrichment analysis showed that the up-regulated DEGs were mainly enriched in the MAPK, PI3K-AKT,

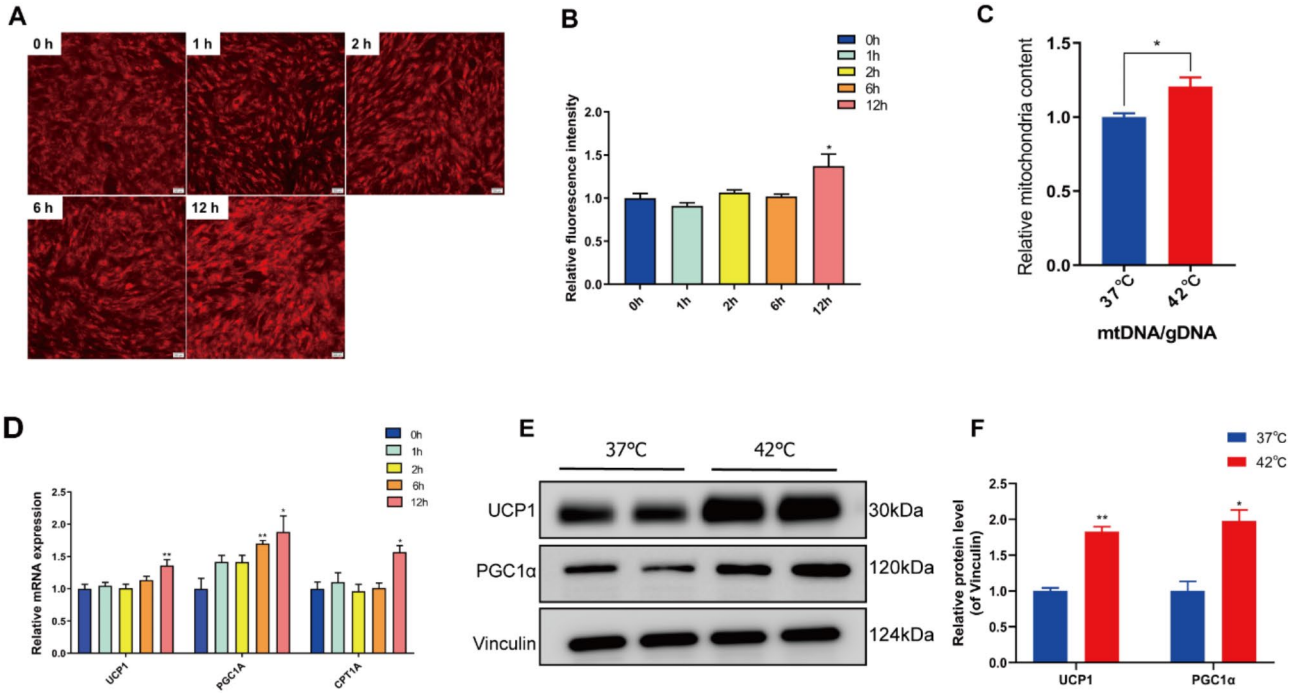

Fig. 3 Heat exposure affects thermogenesis of brown adipocytes. (**A**) Mito-tracker staining of mitochondria in brown adipocytes after different treatment time (scale bar = 200 μm). (**B**) The fluorescence intensity was calculated by ImageJ ($n = 6$); (**C**) Mitochondria DNA content of brown adipocytes in 37℃ and exposed to 42℃ for 12 h ($n = 6$); (**D**) qPCR analysis of thermogenic genes expression of brown adipocytes in 37℃ and exposure to 42℃ for different time ($n = 6$); (**E**) Western blotting of thermogenic proteins of brown adipocytes in 37℃ and 42℃, vinculin was considered as loading control; (**F**) The gray value of UCP1 and PGC1α proteins ($n = 2$). Data are presented as mean ± SEM. *$p < 0.05$ and **$p < 0.01$ versus the corresponding controls are indicated

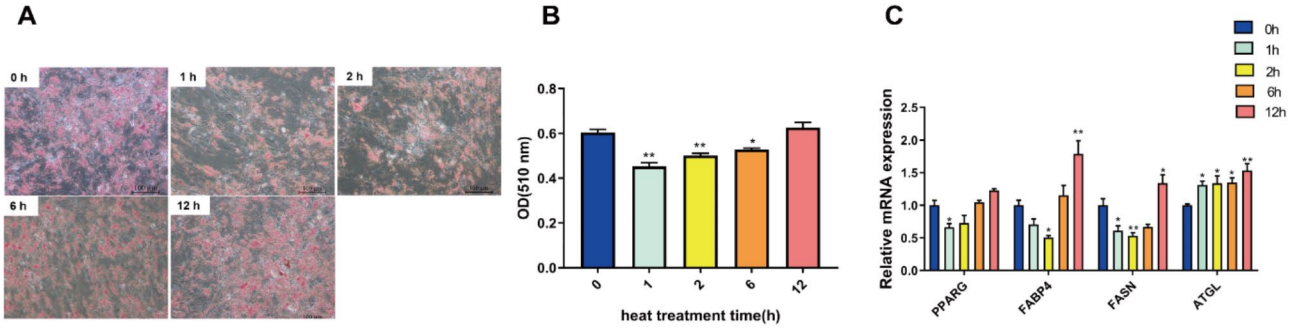

Fig. 4 Heat exposure affects lipogenesis of brown adipocytes. (**A**) Oil Red O staining of brown adipocytes at 37℃ and exposure to 42℃ for different time (scale bar = 200 μm). (**B**) The absorbance of Oil Red O dye at 510 nm was detected ($n = 6$); (**C**) qPCR analysis of lipogenesis genes at 37℃ and exposed to 42℃ for different time ($n = 6$). Data are presented as mean ± SEM. *$p < 0.05$ and **$p < 0.01$ versus the corresponding controls are indicated

hypoxia inducible factor 1, thermogenesis, fatty acid metabolism, and mitophagy-animals pathways (Fig. 5D), and the down-regulated DEGs were mainly enriched in cell cycle, p53 signaling pathway, and rap1signaling pathway (Fig. 5E).

The expression of the heat shock protein family (*HSPAs*, *HSPBs*, and *HSP90*) and genes that respond to heat (*FKBP4*, *HIF3A*, and *STIP1*) were significantly induced after heat exposure (Fig. 6A). The GSEA analysis also indicated that the cellular response to heat pathway was significantly activated (Fig. 6B). Furthermore, we found that the expression of thermogenesis-related genes was increased after heat exposure (Fig. 6C) and adaptive thermogenesis pathway was significantly activated (Fig. 6D). The GSEA analysis also showed that the pathways of adipogenesis (Fig. 6E) and triglyceride catabolism (Fig. 6F) were induced after heat exposure.

Heat exposure promotes mitophagy in goat brown adipocytes

In the KEGG results, mitophagy was a significantly enriched item, therefore we tried to investigate whether heat exposure regulates brown adipocytes thermogenesis through activating mitophagy. We found that

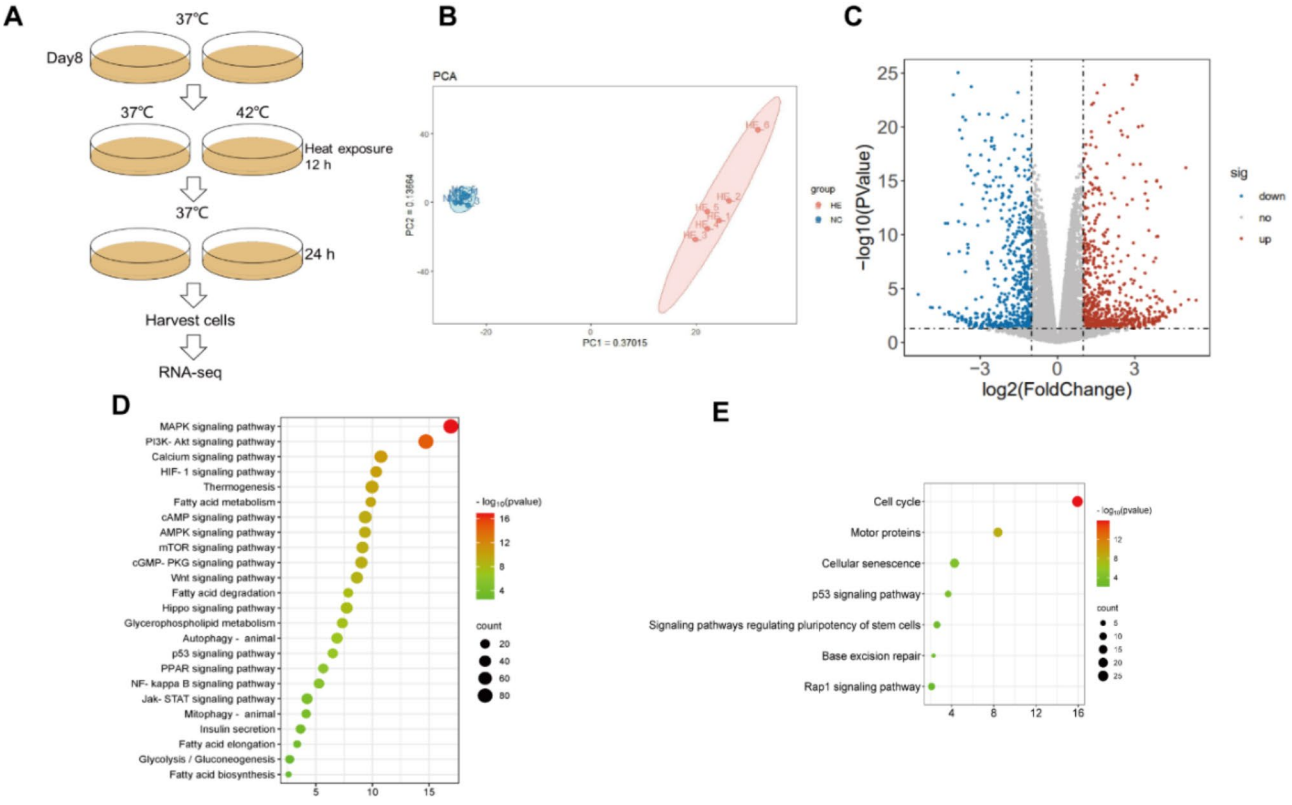

Fig. 5 RNA-seq reveals the effects of heat exposure on goat brown adipocytes. (**A**) Schematic figure of cell culture, 42℃ treatments for 12 h and RNA-seq; (**B**) The PCA plot showed that 37℃ and 42℃ groups were separated into two clusters; (**C**) Differential gene expression profiles between 37℃ and 42℃ group; (**D**) KEGG enrichment analysis for up-regulated DEGs after heat exposure; (**E**) KEGG enrichment analysis for down-regulated DEGs after heat exposure

the expression of mitophagy-related genes (*BNIP3* and *BECN*) was significantly elevated after heat exposure ($p < 0.05$) (Fig. 7A). We further examined autophagy-related protein (LC3B), and mitophagy-related protein (PINK1, BNIP3 and BECN) (Fig. 6B). LC3BII / LC3BI was significantly increased ($p < 0.05$) (Fig. 7C) after heat exposure. In addition, the expression of BNIP3 and BECN proteins was also significantly up-regulated ($p < 0.05$) (Fig. 7D and E) and PINK1 showed no significant change after heat exposure (Fig. 7F). Moreover, the results of transmission electron microscopy (TEM) showed the amounts of autophagosomes and mitophagosomes was increased in heat treatment group (Fig. 7G). These results indicate that heat exposure promotes thermogenesis through activating mitophagy in goat brown adipocytes.

Discussion

Brown adipose tissue (BAT) plays a major role in newborn ruminants to maintain body temperature in the severe cold and the strategies to elevate BAT thermogenesis can reduce the death rate of newborn ruminants [25]. The temperature of external environment directly affects the capacity of thermogenetic adipose tissues. In the prior studies, it has shown that cold exposure induces the thermogenesis of brown [26–28] and beige adipose tissues [29, 30] by activating the hypothalamic-pituitary-adrenal axis. Norepinephrine secreted by the adrenal glands activates the β3-adrenergic receptors on brown adipocytes and up-regulates the expression of thermogenic genes like *UCP1* and *PGC1α* while accelerating lipolysis to promote thermogenesis [31]. Except in cold conditions, the heat stimulation also has an impact on BAT thermogenesis. A recent study has demonstrated that local hyperthermia therapy promotes the thermogenesis of beige adipose in human and mice [16]. In this study, we built the heat exposure model of goat brown adipocytes and results indicated that the thermogenesis capacity was elevated and the level of thermogenesis and adipogenesis genes were also up-regulated. In addition, we also found that the items of thermogenesis, fatty acid degradation in the KEGG enrichment, and triglyceride catabolism in GSEA analysis were highly enriched. Fatty acid is a crucial fuel of thermogenesis [32] and the relationship between fatty acid and thermogenesis after heat exposure is still worth investigating.

In heat exposure experiments, shorter durations of heat treatment can increase body temperature and plasma norepinephrine (NA) levels [33], while the expression

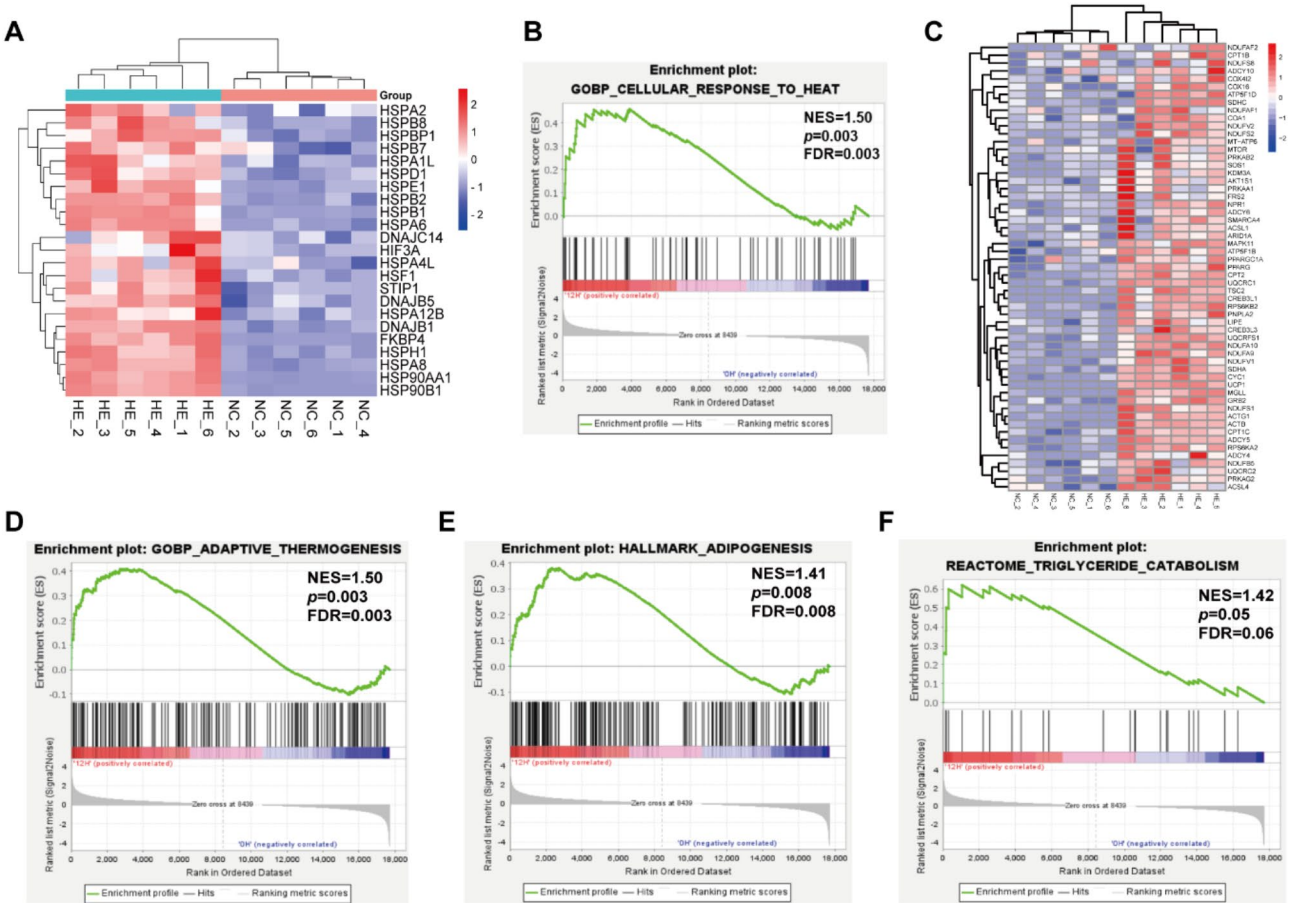

Fig. 6 RNA-seq reveals that heat exposure activates the thermogenesis and adipogenesis of goat brown adipocytes. (**A**) Heat map of TPM values of up-regulated heat shock proteins family genes and genes that respond to heat after heat exposure. (**B**) Gene set enrichment analysis (GSEA) item cellular response to heat was activated by heat exposure; (**C**) Heat map of TPM values of up-regulated thermogenesis related genes after heat exposure; (**D**-**F**) GSEA items adaptive thermogenesis, adipogenesis, and triglyceride catabolism were activated by heat exposure. NES stands for normalized enrichment score

of *UCP1* also elevated after 60 min heat exposure [34]. However, prolonged heat exposure can induce a state of heat stress in animals, which has a broad impact on their physiological functions. Studies have shown that heat stress can disrupt intestinal integrity [35], attenuate appetite [36], and reduce the activity of brown adipose tissue (BAT) [37]. The physiological changes induced by heat stress may affect the functionality of adipocytes, leading to varying thermogenic effects depending on the duration of heat exposure. Therefore, the duration of heat exposure is crucial. It has been reported that a 24 h heat exposure is considered short-term, while 72 h is classified as long-term [38–40]. To investigate the impact of heat exposure on brown adipocytes, we selected different durations for the heat exposure experiment and assessed cell viability. In this study, the chosen of short-term heat exposure (12 h) takes these physiological impacts into account, especially considering the potential inhibitory effects of heat stress on brown adipocyte activity when studying their function.

Previous studies mainly focused on heat exposure in white adipocytes. Prolonged heat exposure performed on adipocytes promotes adipogenic differentiation and lipid accumulation of 3T3-L1 preadipocytes [41] and porcine stromal vascular fractions (SVFs) [42]. Even the ability of adipogenic differentiation of human mesenchymal stromal cells has also been promoted under mild heat stress [23]. In previous studies, heat exposure elevates levels of lipogenesis and induces the expression of lipid-synthesis related genes [43, 44]. On the contrary, short-term heat exposure (also regarded as acute heat exposure) on adipocytes leads to lipolysis and impairs lipogenesis. After 30 and 60 min, 42℃ heat exposure in 3T3-L1 preadipocytes significantly impairs the early adipogenesis [22]. Lipolysis is also promoted after heat exposure for 1 h in bovine adipocytes [24]. In the current study, we found that TG content was decreased at 1 h, 2 h, and 6 h and no differences were observed at 12 h in brown adipocytes. The fall and subsequent rise of TG content is consistent with the expression of lipogenesis genes and lipolysis genes. The results of GSEA analysis also indicated that

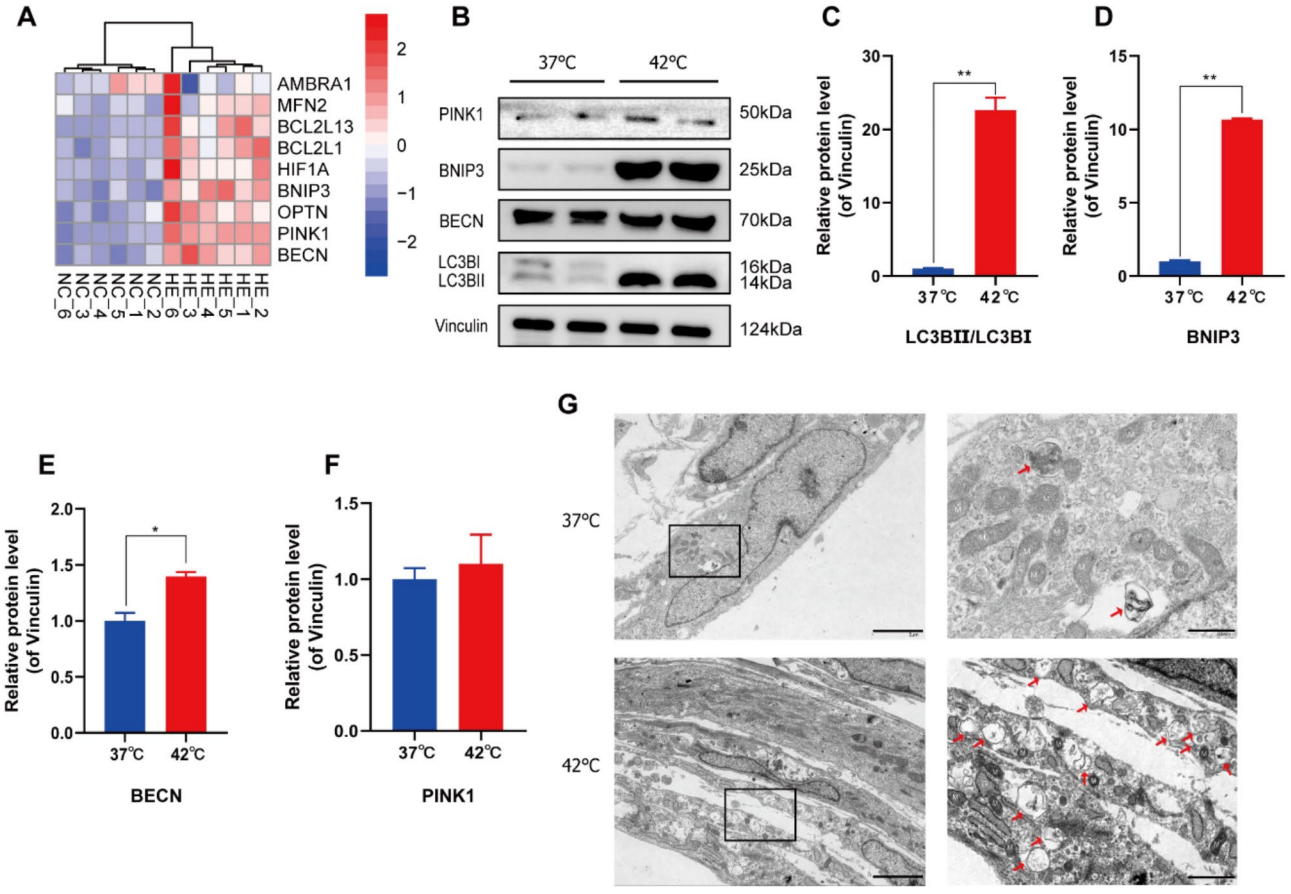

Fig. 7 Heat exposure promotes mitophagy in goat brown adipocytes. (**A**) Heat map of TPM values of up-regulated mitophagy-related genes after heat exposure; (**B**) Western blotting of mitophagy-related proteins brown adipocytes in 37℃ and exposed to 42℃ for 12 h, vinculin was used as loading control ($n = 2$). (**C**-**F**) The gray value of LC3BII/LC3BI, BNIP3, BECN, and PINK1 proteins ($n = 2$). (**G**) Transmission electron micrographs of brown adipocytes after heat exposure (scale bar = left, 2 μm; right, 500 nm; M, mitochondrion; ER, endoplasmic reticulum; N, nuclear; Red arrow, auto/mitophagosome). Data are presented as mean ± SEM. *$p < 0.05$ and **$p < 0.01$ versus the corresponding controls are indicated

the adipogenesis and triglyceride catabolism pathways were activated after 12 h heat exposure, indicating that the lipogenesis and lipolysis are both induced after 12 h heat exposure in goat brown adipocytes.

The capacity of thermogenesis is closely associated with mitochondrial function. Current research indicates that heat exposure impairs the structure and function of mitochondria [45] and creates plenty of damaged mitochondria [46]. Mitophagy is a selective process that wraps and degrades damaged mitochondria. This process maintains mitochondrial homeostasis and normal respiration of cells [47]. It has a pivotal role in thermogenesis and lack of mitophagy impairs the thermogenesis of BAT [48]. However, heat induced mitophagy in brown adipose tissues has not yet been reported. In this study, we found that the mitophagy was induced and the number of mitophagosomes was increased after heat exposure in goat brown adipocytes.

Mitophagy occurs in many organs and tissues to maintain the correct biological process of mitochondria and can be divided into two main pathways, ubiquitin-dependent and ubiquitin-independent pathway [49]. The ubiquitin-dependent pathway relies on massive ubiquitin recruited on the surface of mitochondria, mediated by the interaction of PINK1-Parkin [50]. The ubiquitin-independent pathway, also known as receptor-mediated mitophagy, is mediated by mitochondrial surface receptors, such as BNIP3, BNIP3L, and FUNDC1 [51–53]. In our RNA-seq results, the mitophagy pathway was induced. Then, we tried to figure out whether the mitophagy occurred and which kind of mitophagy was the primary pathway in heat exposed goat brown adipocytes. Therefore, we determined mitophagy-related effectors including LC3B, PINK1, and BNIP3. The protein level of PINK1 has no difference changes after heat exposure. However, the protein level of BNIP3 was induced and the LC3BII/LC3BI ratio was significantly elevated after heat treatment. These results support that the BNIP3-mediated mitophagy was induced by heat treatment. Therefore, the BNIP3-mediated mitophagy occurring in goat brown adipocytes may be a cellular response to heat treatment.

In neonatal goat kids, brown adipose tissue (BAT) is essential for thermogenesis and maintaining body temperature, as they have limited thermoregulation ability after birth [1]. BAT activation is particularly crucial during the early postnatal period to protect against cold [54]. Based on our research, we found that short-term heat exposure can activate thermogenesis in brown adipocytes. This finding provides insights for the postnatal care of neonatal goats. By implementing short-term heat exposure strategies, we can enhance the thermogenic capacity of neonatal goats, thereby improving their cold resistance. Finally, there were some limitations to our research. The RNA-seq analysis was conducted at the 12 h time point, longer time points were not included, and we did not further evaluate cell vitality changes between the 12 h and 24 h heat exposure. Furthermore, our study used female neonatal goats, and the potential impact of sex differences on the results remains unaddressed. We will focus on the longer duration of heat exposure and sex differentiation in future research.

Conclusion

This study was designed to identify the effect of heat exposure on goat brown adipocytes. These results indicate that the lipogenesis and lipolysis of brown adipocytes were induced after 12 h heat exposure. In addition, heat exposure promoted the thermogenesis through activating mitophagy in goat brown adipocytes. This study inspires us that heat exposure has the potential to improve thermogenesis in goat kids and has implications for postnatal care strategies in neonatal goats. Our study presents evidence supporting the role of heat exposure in the adaptive thermogenesis regulation of goat brown adipocytes.

Materials and methods

Experimental animals

All Chuanzhong black goats were maintained at the breeding center of Sichuan Agricultural University, Ya'an, China. We chose three female newborn goat kids, which were delivered by three ewes at the same day (body weight 2.4 ± 0.2 kg). The goat kids were wiped and fed colostrum (30 mL/kg BW). After 24 h, these goat kids were injected with su mian xin (0.1mL/kg BW, Shengda, Changchun, China), and sacrificed by arterial bleeding under full anesthesia.

Brown adipose-derived stromal vascular fractions (SVFs) isolation and culture

The stromal vascular fractions (SVFs) were separated from the perirenal brown adipose tissues of the above three female Chuanzhong black goats, minced and digested with 0.1% collagenase I in HBSS buffer supplemented with 2% penicillin-streptomycin at 37 °C for 1 h. To neutralize the collagenase, an equal volume of DMEM/F-12 medium containing 2% penicillin-streptomycin and 15% fetal bovine serum (FBS) was added. The digested tissue was then filtered through a 100 μm cell strainer, followed by centrifugation at 500 × g for 5 min. The cell pellets were resuspended in DMEM/F-12 medium containing 1% penicillin-streptomycin and 10% FBS, filtered through a 40 μm cell strainer. Then, SVFs were suspended in DMEM/F12 with 10% FBS and incubated at 37℃ with 5% CO_2.

Brown adipocytes differentiation and heat treatments

After 2 days of complete confluence, 1 μM rosiglitazone, 850 nM insulin, 1 nM triiodothyronine, 0.5 mM IBMX, and 5 μM dexamethasone were added into DMEM/F12 with 10% FBS to induce the SVFs to differentiate to brown adipocytes. The differentiation medium was replaced with maintenance medium (DMEM/F12 added 10% FBS, 1 μM rosiglitazone, 1 nM triiodothyronine, and 850 nM insulin) after two days. On the eighth day, brown adipocytes were treated at 37℃ (NC) or 42℃ (HE). The HE groups suffered different heat treatment times, as 1, 2, 6, and 12 h. After heat treatments, cells were returned to 37℃ with 5% CO_2 incubator for 24 h, then the cells were harvested. The cell culture schema is listed in Table S3.

RNA isolation and qPCR

Total RNA was isolated from brown adipocytes using RNAiso (TAKARA, Tokyo, Japan), a reagent that efficiently extracts high-quality RNA using a guanidine thiocyanate-based method, protecting RNA from degradation. Adipocytes were exposed to 42℃ heat treatment for 1, 2, 6, and 12 h, followed by recovery at 37℃ 24 h, and then lysed using RNAiso reagent for RNA extraction with chloroform. RNA was then precipitated with isopropanol, washed with ethanol, and air-dried. Finally, the RNA was dissolved in nuclease-free water and the concentration was determined by NanoDrop 2000 (Thermo, MA, USA). The concentration and integrity of RNA are listed in Table S4 and Fig S2A. Subsequently, 1 μg of total RNA was reverse transcribed to cDNA by HiScript III 1st Strand cDNA Synthesis Kit (Vazyme, Nanjing, China) for subsequent qPCR analysis. *GAPDH* and *PFDN5* served as reference genes to normalize gene expression levels following the $2^{-\Delta\Delta Ct}$ method. Primer sequences are shown in the primer list (Table S1).

Cellular viability determination

Cells were cultured in cell incubator with 5% CO_2 for 8 days before undergoing different durations of 42 °C heat treatment. Subsequently, the cells were returned to 37 °C for 24 h. After that, the cell viability was assessed by the CCK-8 kit (SK2060, Coolaber, Beijing, China). The

CCK-8 was added into medium and incubated at 37℃ for 1 h, then assess the cell viability through absorbance measurement at 450 nm.

Mitochondrial content determination

The TIANamp Genomic DNA Kit (Tiangen, Beijing, China) was employed for isolating total DNA from brown adipocytes. Briefly, brown adipocytes were lysed with the provided lysis buffer, and the DNA was purified by passing the lysate through a silica-based membrane to remove contaminants. The extracted DNA was then eluted in the provided elution buffer and stored at -20 °C. DNA concentration was determined by NanoDrop 2000. The concentration and integrity of DNA was listed in Table S5 and Fig S2B. The mitochondria content was measured by qPCR analysis. The Ct value ratio of mitochondrial *D-loop* to nuclear *TBP* was considered the relative content of mitochondria.

Mitotracker stain

Adipocytes were stained with the solution containing Mito-Tracker Red CMXRos (1:5000, Beyotime, Shanghai, China) and incubated under cell culture condition for 30 min. After that, we observed the cells under an electron microscope at 579 nm.

Oil red O staining

After heat exposure, brown adipocytes were fixing with 4% paraformaldehyde. The paraformaldehyde was discarded after 30 min and 60% isopropanol was added for 2 min. Cells was stained with diluted oil red O solution for 30 min, followed by washing the excess solution with distilled water. Finally, the oil red O dye was further diluted with 100% isopropanol and measured the absorbance at 490 nm.

Western blotting

Total protein was obtained by Bestbio Total Protein Extraction Kit (BB-3101, Bestbio, Shanghai, China) from brown adipocytes. The adipocytes were washed with PBS and lysed using a lysis buffer containing protease inhibitors and phosphatase inhibitors. Then the lysates were centrifuged at 4 °C, 12,000×g for 15 min. The supernatant was collected as the protein sample. The concentration of protein was detected with Bicinchoninic Acid (BCA) method. The 20μL protein samples were mixed with BCA working solution and incubated at 37℃ for 30 min, then measured the absorbance at 562 nm. Equal amounts of protein are mixed with SDS sample buffer and electrophoresis was performed on a 10% SDS-PAGE gel. Proteins were transferred from the gel onto a polyvinylidene fluoride (PVDF) membranes and blocked with 5% non-fat milk powder in TBST. The rabbit primary antibodies were diluted to 1:500 for anti-UCP1 (Cell Signaling Technology, MA, USA), 1:1000 for anti-Vinculin, anti-PGC1α, anti-BNIP3, anti-PINK1 and anti-BECN (Abclonal, Wuhan, China), 1:500 for anti-LC3B (Abclonal, Wuhan, China) and the secondary antibody was diluted to 1:1000 for HPR-labeled goat anti-rabbit IgG (Abclonal, Wuhan, China). At last, we used BeyoECL Plus detection system (Beyotime, Shanghai, China) and a ChemiDoc Imaging Systems (Bio-Rad, CA, USA) to determine target proteins. The bands of target protein were quantified with ImageJ [55] through calculating gray value intensity. The whole membrane images were shown in Fig. S1.

Immunocytochemistry and BODIPY staining

The adipocytes were fixed for 15 min as previously described and treated with 0.25% Triton X-100 for 10 min. After three times washing with PBS, cells were incubated overnight at 4 °C with primary antibodies: rabbit anti-UCP1 (1:100, Cell Signaling Technologies). Following this, cells were treated with secondary antibody Cy3 goat Anti-Rabbit IgG (1:500, Abclonal, Wuhan, China) at 37 °C for 1 h. At last, adipocytes were stained 5 μM BODIPY (Invitrogen, CA, USA) with DAPI (Beyotime, Shanghai, China) and inspected under fluorescence microscopic observation.

RNA-seq library construction and sequencing

Total RNA was isolated from the brown adipocytes following exposure at 37–42 °C using RNAiso (TAKARA, Tokyo, Japan). Total RNA concentration was determined with NanoDrop 2000 (Thermo, MA, USA). The mRNA was enriched from total RNA using poly-T oligo-attached magnetic beads and then synthesized double-stranded cDNA. We constructed a total of 12 RNA-seq libraries across two groups: control group (37 °C) and heat exposure group (42 °C), ensuring 6 biological replicates for each group. The 12 different libraries were prepared to compare the gene expression profiles between the control (37 °C) and heat-exposed (42 °C) groups. After purification, the sequencing was performed using the PE150 strategy on Illumina Novaseq6000 platform at Novogene Bioinformatics Technology Co., Ltd (Beijing, China). Summary statistics of RNA-seq sequencing data are listed in Table S2.

RNA-seq analysis procedure

Raw data were screened out all low-quality reads to obtain clean data. After that, HISAT2 (v2.2.1) [56] was employed to align clean reads to the goat reference genome (ARS1.2). Aligned data were assembled and qualified. Differential expressed genes were analyzed by edgeR [57] and the significance of differential expressed genes was set at $p < 0.05$ and|Log (fold change)| > 1. At last, GO and KEGG were employed for genes functional

annotation and enrichment analysis through Metascape (http://metascape.org/ (accessed on 15 May 2023)), $p < 0.05$ was considered significant enrichment. GSEA analysis was conducted with GSEA software (v4.3.2, https://www.gsea-msigdb.org/gsea/index.jsp).

Transmission electron microscopy

Adipocytes were washed with 0.1 M phosphate buffer (PB) (pH 7.4) and fixed with 2.5% glutaraldehyde for 2 h, followed by gentle scraping with a cell scraper. Subsequently, adipocytes were washed twice in 0.1 M PB and then fixed in 1% osmic acid for 1 h. Dehydration was achieved through a concentration gradient of ethanol and acetone before embedding the cells in 812 epoxy resins (Sigma-Aldrich, MO, USA). 60 nm ultrathin sections were sliced from the blocks and stained with 2% uranyl acetate and 2.6% lead citrate, respectively. Finally, the HT7800 transmission electron microscope (HITACHI, Tokyo, Japan) was employed to observe the sections.

Statistical analysis

All quantitative data are presented as mean ± SEM, analyzed and visualized with GraphPad Prism 8.0. The unpaired Student's t test was used for comparing two groups, while one-way ANOVA with Tukey's multiple comparisons was employed to compare multiple groups. $p < 0.05$ was assumed as significant and $p < 0.01$ was assumed as extremely significant.

Abbreviations

BAT	Brown adipose tissue
WAT	White adipose tissue
UCP1	Uncoupling protein 1
PGC1α	PPARG Coactivator 1 Alpha
CPT1A	Carnitine Palmitoyltransferase 1 A
ELOVL3	Elongation Of Very Long Chain Fatty Acids Protein 3
ELOVL6	Elongation Of Very Long Chain Fatty Acids Protein 6
HSP	Heat shock protein
HSF	Heat shock factor
FKBP4	FKBP Prolyl Isomerase 4
STIP1	Stress Induced Phosphoprotein 1
HIF3A	Hypoxia Inducible Factor 3 Subunit Alpha
PPARγ	Peroxisome Proliferator Activated Receptor Gamma
FABP4	Fatty Acid Binding Protein 4
FASN	Fatty Acid Synthase
ATGL	Patatin Like Phospholipase Domain Containing 2
LC3B	Microtubule Associated Protein 1 Light Chain 3 Beta
BECN	Beclin 1
PINK1	PTEN Induced Putative Kinase 1
BNIP3	BCL2 Interacting Protein 3
BNIP3L	BCL2 Interacting Protein 3 Like
FUNDC1	FUN14 Domain Containing 1
TBST	Tris-buffered saline with Tween 20
PCA	Principal Component Analysis
PB	phosphate buffer

Supplementary Information

The online version contains supplementary material available at https://doi.org/10.1186/s12864-025-11467-3.

Supplementary Material 1
Supplementary Material 2
Supplementary Material 3
Supplementary Material 4
Supplementary Material 5
Supplementary Material 6
Supplementary Material 7
Supplementary Material 8

Acknowledgements

Not applicable.

Author contributions

YS: Conceptualization, Methodology, Visualization, Writing– original draft. DL: Data curation, Formal analysis. DS: Formal analysis, Software. TJ: Formal analysis. LL: Visualization. SZ: Investigation, Project administration. JC: Data curation, Software. LL: Resources. HZ: Resources. TZ: Software Validation. JG: Data curation Software. LW: Funding acquisition, Project administration, Supervision.

Funding

This work was supported by the grant from the Key Research and Development Program in Xizang (No. XZ202401ZY0083) and the National College Student Innovation and Entrepreneurship Training Program (No. 202310626002).

Data availability

The raw sequence data reported in this paper have been deposited in the Genome Sequence Archive [58] in National Genomics Data Center [59], China National Center for Bioinformation/Beijing Institute of Genomics, Chinese Academy of Sciences (GSA: CRA017624) that are publicly accessible at https://ngdc.cncb.ac.cn/gsa.

Declarations

Ethics approval and consent to participate

All methods were conducted in compliance with the Regulations for the Administration of Affairs Concerning Experimental Animals (Ministry of Science and Technology, China, revised March 2017). In this study, all animal research was conducted following the guidelines established by the Institutional Animal Care and Use Committee of Sichuan Agricultural University, under permit No. DKY-2022202016.

Consent for publication

Not applicable.

Competing interests

The authors declare no competing interests.

Received: 23 September 2024 / Accepted: 10 March 2025
Published online: 19 March 2025

References

1. Symonds ME, Pope M, Budge H. The ontogeny of brown adipose tissue. Annu Rev Nutr. 2015;35:295–320.
2. Lidell M, Betz M, Enerbäck SJ. Brown adipose tissue and its therapeutic potential. J Intern Med. 2014;276(4):364–77.
3. Basse AL, Dixen K, Yadav R, Tygesen MP, Qvortrup K, Kristiansen K, Quistorff B, Gupta R, Wang J, Hansen JB. Global gene expression profiling of brown to white adipose tissue transformation in sheep reveals novel transcriptional components linked to adipose remodeling. BMC Genomics. 2015;16(1):215.
4. Wang Y, Chen X, Fan W, Zhang X, Zhan S, Zhong T, Guo J, Cao J, Li L, Zhang H, et al. Integrated application of metabolomics and RNA-seq

reveals thermogenic regulation in goat brown adipose tissues. FASEB J. 2021;35:e21868.
5. Liu X, Zhu Y, Zhan S, Zhong T, Guo J, Cao J, Li L, Zhang H, Wang L. RNA-Seq reveals MiRNA role in thermogenic regulation in brown adipose tissues of goats. BMC Genomics. 2022;23:186.
6. Harms M, Seale P. Brown and beige fat: development, function and therapeutic potential. Nat Med. 2013;19(10):1252–63.
7. Alexander G, McCance I. Temperature regulation in the new-born lamb. I. Changes in rectal temperature within the first six hours of life. Aust J Agric Res. 1958;9(3):339–47.
8. Stafford KJ, Kenyon PR, Morris ST, West DM. The physical state and metabolic status of lambs of different birth rank soon after birth. Livest Sci. 2007;111(1):10–5.
9. Gordon R, Brien FD, Hinch GN, van de Remy V. Neonatal lamb mortality: factors associated with the death of Australian lambs. Anim Prod Sci. 2016;56(4):726–35.
10. Plush KJ, Brien FD, Hebart ML, Hynd PI. Thermogenesis and physiological maturity in neonatal lambs: a unifying concept in lamb survival. Anim Prod Sci. 2016;56(4):736–45.
11. Symonds ME, Budge H, Perkins AC, Lomax MA. Adipose tissue development–impact of the early life environment. Prog Biophys Mol Biol. 2011;106(1):300–6.
12. Liu X, Tang J, Zhang R, Zhan S, Zhong T, Guo J, Wang Y, Cao J, Li L, Zhang H, et al. Cold exposure induces lipid dynamics and thermogenesis in brown adipose tissue of goats. BMC Genomics. 2022;23(1):528.
13. Xin L, Wenli F, Xujia Z, Siyuan Z, Tao Z, Jiazhong G, Yan W, Jiaxue C, Li L, Hongping Z, et al. Maternal L-carnitine supplementation promotes brown adipose tissue thermogenesis of newborn goats after cold exposure. FASEB J. 2022;36(8):e22461.
14. Stephen BS, Craig RS, Carstens GE. Supplementary prenatal copper increases plasma Triiodothyronine and brown adipose tissue uncoupling protein-1 gene expression but depresses thermogenesis in newborn lambs. Asian-Australasian J Anim Sci. 2020;33(3):506–14.
15. Sorin MM, Rebecca MS, Guoyao W, Satterfield MC. Maternal arginine supplementation enhances thermogenesis in the newborn lamb. J Anim Sci. 2020;98(5):118.
16. Li Y, Wang D, Ping X, Zhang Y, Zhang T, Wang L, Jin L, Zhao W, Guo M, Shen F, et al. Local hyperthermia therapy induces Browning of white fat and treats obesity. Cell. 2022;185(6):949–e966919.
17. Pearce SC, Sanz Fernandez MV, Torrison J, Wilson ME, Baumgard LH, Gabler NK. Dietary organic zinc attenuates heat stress-induced changes in pig intestinal integrity and metabolism. J Anim Sci. 2015;93(10):4702–13.
18. Jason WR, Benjamin JH, Seibert JT, Malavika KA, Aileen FK, Lance HB. Physiological mechanisms through which heat stress compromises reproduction in pigs. Mol Reprod Dev. 2017;84(9):934–45.
19. Okabe K, Uchiyama S. Intracellular thermometry uncovers spontaneous thermogenesis and associated thermal signaling. Commun Biology. 2021;4(1):1377.
20. Dewal RS, Yang FT, Baer LA, Vidal P, Hernandez-Saavedra D, Seculov NP, Ghosh A, Noé F, Togliatti O, Hughes L, et al. Transplantation of committed pre-adipocytes from brown adipose tissue improves whole-body glucose homeostasis. iScience. 2024;27(2):108927.
21. Bernabucci U, Basirico L, Morera P, Lacetera N, Ronchi B, Nardone A. Heat shock modulates adipokines expression in 3T3-L1 adipocytes. J Mol Endocrinol. 2009;42(2):139–47.
22. Ezure T, Amano S. Heat stimulation reduces early adipogenesis in 3T3-L1 preadipocytes. Endocrine. 2009;35(3):402–8.
23. Choudhery MS, Badowski M, Muise A, Harris DT. Effect of mild heat stress on the proliferative and differentiative ability of human mesenchymal stromal cells. Cytotherapy. 2015;17(4):359–68.
24. Faylon MP, Baumgard LH, Rhoads RP, Spurlock DM. Effects of acute heat stress on lipid metabolism of bovine primary adipocytes. J Dairy Sci. 2015;98(12):8732–40.
25. Slee J. The effects of breed, birthcoat and body weight on the cold resistance of newborn lambs. Anim Sci. 1978;27(1):43–9.
26. vML WD, GJ JWVNMSJMD, ND K, GJ BPS. Cold-activated brown adipose tissue in healthy men. N Engl J Med. 2009;360(15):1500–8.
27. Smith RE, Roberts JC. Thermogenesis of brown adipose tissue in cold-acclimated rats. Am J Physiol. 1964;206:143–8.
28. Griggio MA. Thermogenic mechanisms in cold-acclimated animals. Brazilian J Med Biol Res = Revista Brasileira De Pesquisas Medicas E Biologicas. 1988;21(2):171–6.
29. Fan H, Zhang Y, Zhang J, Yao Q, Song Y, Shen Q, Lin J, Gao Y, Wang X, Zhang L, et al. Cold-Inducible Klf9 regulates thermogenesis of brown and beige fat. Diabetes. 2020;69(12):2603–18.
30. Yao L, Cui X, Chen Q, Yang X, Fang F, Zhang J, Liu G, Jin W, Chang Y. Cold-Inducible SIRT6 regulates thermogenesis of brown and beige fat. Cell Rep. 2017;20(3):641–54.
31. Cannon B, Nedergaard J. Brown adipose tissue: function and physiological significance. Physiol Rev. 2004;84(1):277–359.
32. Jieun L, Jessica ME, Michael JW. Adipose fatty acid oxidation is required for thermogenesis and potentiates oxidative Stress-Induced inflammation. Cell Rep. 2015;10(2):266–79.
33. Nishant Ranjan C, Medha K, Laxmi Prabha S, Rajinder KG, Ramesh Chand M, Rajkumar T, Sarita N, Shashi Bala S. Heat stress-induced neuroinflammation and aberration in monoamine levels in hypothalamus are associated with temperature dysregulation. Neuroscience. 2017;358(6):79–92.
34. Suzuki K, Yamaga H, Ohtaki H, Hirako S, Miyamoto K, Nakamura M, Yanagisawa K, Shimada T, Hosono T, Hashimoto H et al. Effect of PACAP on heat exposure. 2023, 24(4):3992.
35. Sarah P, Venkatesh M, Rebecca LB, Jay SJ, Thomas W, Jason WR, Robert PR, Lance HB, Nicholas KG. Heat stress reduces intestinal barrier integrity and favors intestinal glucose transport in growing pigs. PLoS ONE. 2013;8(8):e70215–70215.
36. Sarah P, Sanz-Fernandez MV, James H, Lance HB, Nicholas KG. Short-term exposure to heat stress attenuates appetite and intestinal integrity in growing pigs1. J Anim Sci. 2014;92(12):5444–54.
37. Penghua L, Lin-Lin Z, Qi Y, Jie R, Xiaoming S, Biying Z, Liuyi W, Shiduan C, Sijia L, Hongli Z, et al. Heat stress reduces brown adipose tissue activity by exacerbating mitochondrial damage in type 2 diabetic mice. J Therm Biol. 2024;119:103799.
38. Sharif Hasan S, Sivakumar Allur S, Darae K, Jinryong P, Mousumee K, Hyun Woo C, Kwan Seob S. Direct exposure to mild heat stress stimulates cell viability and heat shock protein expression in primary cultured broiler fibroblasts. Cell Stress Chaperones. 2020;25(6):1033–43.
39. Chun-qi G, Yongmei Z, Hai-chang L, Sui WG, Huichao Y, Xiuqi W. Heat stress inhibits proliferation, promotes growth, and induces apoptosis in cultured Lantang swine skeletal muscle satellite cells. J Zhejiang University-SCIENCE B. 2015;16(6):549–59.
40. Jinryong P, Jeongeun L, Kwan Seob S. Effects of heat stress exposure on Porcine muscle satellite cells. J Therm Biol. 2023;114:103569.
41. Huang Y, Xie H, Pan P, Qu Q, Xia Q, Gao X, Zhang S, Jiang Q. Heat stress promotes lipid accumulation by inhibiting the AMPK-PGC-1alpha signaling pathway in 3T3-L1 preadipocytes. Cell Stress Chaperones. 2021;26(3):563–74.
42. Qu H, Donkin SS, Ajuwon KM. Heat stress enhances adipogenic differentiation of subcutaneous fat depot–derived Porcine stromovascular cells. J Anim Sci. 2015;93:3832–42.
43. Qu H, Yan H, Lu H, Donkin S, Ajuwon S. Heat stress in pigs is accompanied by adipose tissue–specific responses that favor increased triglyceride storage. J Anim Sci. 2016;94:1884–96.
44. Heng J, Tian M, Zhang W, Chen F, Guan W, Zhang S. Maternal heat stress regulates the early fat deposition partly through modification of m(6)A RNA methylation in neonatal piglets. Cell Stress Chaperones. 2019;24(3):635–45.
45. Huang C, Jiao H, Song Z, Zhao J, Wang X, Lin H. Heat stress impairs mitochondria functions and induces oxidative injury in broiler chickens. J Anim Sci. 2015;93(5):2144–53.
46. Lu J, Li H, Yu D, Zhao P, Liu Y. Heat stress inhibits the proliferation and differentiation of myoblasts and is associated with damage to mitochondria. Front Cell Dev Biology. 2023;11:1171506.
47. Palikaras K, Lionaki E, Tavernarakis N. Mechanisms of mitophagy in cellular homeostasis, physiology and pathology. Nat Cell Biol. 2018;20(9):1013–22.
48. Ko MS, Yun JY, Baek IJ, Jang JE, Hwang JJ, Lee SE, Heo SH, Bader DA, Lee CH, Han J, et al. Mitophagy deficiency increases NLRP3 to induce brown fat dysfunction in mice. Autophagy. 2021;17(5):1205–21.
49. Lu Y, Li Z, Zhang S, Zhang T, Liu Y, Zhang L. Cellular mitophagy: mechanism, roles in diseases and small molecule Pharmacological regulation. Theranostics. 2023;13(2):736–66.
50. Ghazaleh A, Thomas LS. The pathways of mitophagy for quality control and clearance of mitochondria. Cell Death Differ. 2012;20:31–42.
51. Paul AN. Mitochondrial autophagy: origins, significance, and role of BNIP3 and NIX. Biochim Et Biophys Acta Mol Cell Res. 2015;1853(10):2775–83.
52. Ziheng C, Lei L, Qi C, Yanjun L, Hao W, Weilin Z, Yueying W, Sheikh Arslan S, Sami S, Xiaohui W, et al. Mitochondrial E3 ligase MARCH 5 regulates FUNDC 1 to fine-tune hypoxic mitophagy. EMBO Rep. 2017;18:495–509.

53. Ivana N, Vladimir K, David GM, Ji Z, Philipp SW, Alexis R, Vladimir VR, Frank L, Doris P, Angelo O, et al. Nix is a selective autophagy receptor for mitochondrial clearance. EMBO Rep. 2009;11:45–51.
54. Alexander G, Bell AW, Hales JRS. Effects of cold exposure on tissue blood flow in the new-born lamb. J Physiol. 1973;234:65–77.
55. Schneider CA, Rasband WS, Eliceiri KW. NIH image to imageJ: 25 years of image analysis. Nat Methods. 2012;9(7):671–5.
56. Kim D, Paggi JM, Park C, Bennett C, Salzberg SL. Graph-based genome alignment and genotyping with HISAT2 and HISAT-genotype. Nat Biotechnol. 2019;37(8):907–15.
57. Chen Y, Lun ATL, Smyth GK. From reads to genes to pathways: differential expression analysis of RNA-Seq experiments using Rsubread and the edger quasi-likelihood pipeline. F1000Research. 2016;5:1438.
58. Chen T, Chen X, Zhang S, Zhu J, Tang B, Wang A, Dong L, Zhang Z, Yu C, Sun Y, et al. The genome sequence archive family: toward explosive data growth and diverse data types. Genom Proteom Bioinform. 2021;19(4):578–83.
59. Members C-N, Partners. Database resources of the National genomics data center, China National center for bioinformation in 2022. Nucleic Acids Res. 2022;50(D1):D27–38.

Publisher's note